Delivery of high-stability optical and microwave frequency standards over an optical fiber network

Jun Ye,* Jin-Long Peng,¶ R. Jason Jones, Kevin W. Holman, John L. Hall, and David J. Jones

JILA, National Institute of Standards and Technology and University of Colorado, Boulder, Colorado 80309-0440

Scott A. Diddams, John Kitching, Sebastien Bize, James C. Bergquist, and Leo W. Hollberg

Time and Frequency Division, National Institute of Standards and Technology, 325 Broadway, Boulder, Colorado 80305

Lennart Robertsson and Long-Sheng Ma

Bureau International des Poids et Mesures, Pavillon de Breteuil, 92312 Sevres, France

Received October 16, 2002; revised manuscript received February 11, 2003

Optical and radio frequency standards located in JILA and National Institute of Standards and Technology (NIST) laboratories have been connected through a 3.45-km optical fiber link. An optical frequency standard based on an iodine-stabilized Nd:YAG laser at 1064 nm (with an instability of $\sim 4 \times 10^{-14}$ at 1 s) has been transferred from JILA to NIST and simultaneously measured in both laboratories. In parallel, a hydrogen maser-based radio frequency standard (with an instability of $\sim 2.4 \times 10^{-13}$ at 1 s) is transferred from NIST to JILA. Comparison between these frequency standards is made possible by the use of femtosecond frequency combs in both laboratories. The degradation of the optical and rf standards that are due to the instability in the transmission channel has been measured. Active noise cancellation is demonstrated to improve the transfer stability of the fiber link. © 2003 Optical Society of America

OCIS codes: 120.0120, 060.0060, 120.3930, 140.7090, 120.5050.

1. INTRODUCTION

The stability of the best microwave and optical frequency standards, for times less than approximately one week, can now exceed the capabilities of the traditional transmission systems [i.e., Global Positioning System (GPS), two-way time transfer] used to distribute these time and frequency reference signals to remote sites. The instabilities in transmission channels can contribute a significant fraction of the overall uncertainty in the comparison of high-performance standards that are not collocated.[1] This fact has been occasionally used as a counterargument against further development of frequency standards that have higher stabilities. Although improvement in the transfer process over large-scale signal paths remains challenging, researchers have been experimenting with optical fibers as effective means for local networks of dissemination or comparison of time and frequency standards, both in the microwave and optical domains. The attractiveness of this approach lies in the fact that an environmentally isolated fiber can be considerably more stable than open-air paths, especially at short time scales. Furthermore, the same advantages enjoyed by communication systems in optical fiber (e.g., low loss and scalability) can be realized in a time and frequency distribution system. Active stabilization of fiber-optic channels for the distribution of reference frequencies can also be employed to improve the stability of the transmitted standard. Besides the obvious benefit of more precise time and frequency transfer, an actively stabilized optical fiber network can play a critical role in the implementation of long-baseline coherent interferometry.

As the first example, NASA's Deep Space Network requires distribution of ultrastable reference frequencies from their Signal Processing Center at the Jet Propulsion Laboratory to multiple antenna sites for the gravity wave searches, occultation science, and other radio science experiments.[2] In that work, a stabilized fiber-optic distribution system was developed for microwave frequency dissemination. An optical carrier was amplitude modulated with the rf standard and sent to the remote site through the fiber link. Environmental perturbations on the fiber, such as vibration or temperature variation, introduced group-delay variations and degraded the frequency stability of the rf standard. To eliminate the induced fiber noise actively, a signal was sent back to the transmitting site with proper coding to distinguish the round-trip signal from the launched one. The round-trip rf signal contained the fiber-induced noise and was used to derive an error signal to control the group delay of the transmitted path by use of a temperature-compensated fiber reel. Instability of parts in 10^{14} at 1 s was achieved for a 16-km-long fiber buried 1.5 m beneath the Earth's surface. A cryogenic sapphire oscillator was needed at the remote site for the short-term requirement, as an in-

stability of approximately 5×10^{-15} at 1 s is required for the desired gravitational wave searches.

Time transfer over a 200-km optical fiber plant between Phoenix and Tucson, Arizona, was also recently realized with subpicosecond rms fluctuations over a 3.5-day period.[3] In this study the optical carrier was a 1.55-μm laser diode and the time information was encoded by amplitude modulation of the diode with a 155.52-MHz rf signal [corresponding to the OC-3 synchronous optical network (SONET) frequency]. Similar to the NASA study, a portion of the signal at the receiver was returned to the transmitter, where the phase differences between the original and the (round-trip) transmitted signal were measured in the electrical domain. Based on these phase differences, the overall time delay was actively controlled to compensate for fluctuations in the optical path length of the fiber. This optical-based approach was found to be superior to remote steering of time by means of a tunable frequency synthesizer at the receiver end.

Optical frequency standards have also been transferred through an optical fiber. Real-time sensing of the fiber-induced phase noise and active servo control of up to a few kilohertz bandwidth were sufficient to suppress the optical phase noise completely and to maintain a millihertz level tracking capability between the optical carriers at the two ends of a 25-m-long polarization-maintaining fiber located in our JILA laboratory.[4] A similar approach was adopted in the laboratory of Bergquist at NIST to deliver hertz-linewidth laser light for the study of a single-mercury ion-based optical frequency standard.[5,6] This optical frequency standard is connected to a femtosecond comb-based frequency measurement system by means of a 180-m-long fiber located inside the NIST building.[7] Without an active phase-noise-cancellation feedback system, the laser linewidth transmitted through an optical fiber will certainly experience broadening; however, the accumulated frequency shift over an extended averaging period was determined to be less than 3 Hz over a 3-km-long fiber.[8] With the recent demonstration of optical atomic clocks,[9,10] interest in the development of highly stable and accurate optical fiber transmission networks has become stronger, for obvious reasons: the unprecedented stability promised by optical frequency standards will need direct optical links for distribution and intercomparison.

We report our recent research in transmitting and comparing highly stable rf and optical frequency standards by using two installed dark fibers in the Boulder Research and Administrative Network (BRAN).[11] The optical link between the laboratories located, respectively, in JILA and the National Institute of Standards and Technology (NIST) Boulder is a 6.9-km-long round trip. A hydrogen maser-based rf standard with an instability of $\sim 2.4 \times 10^{-13}$ at 1 s is transferred from NIST to JILA. This maser-based rf reference, approximately ten times more stable than a commercial Cs atomic clock in JILA, is used as the time base for femtosecond-laser-based optical combs used for absolute optical frequency measurements.[12] The maser-based signal is also used to make direct comparisons against the output of an optical clock, i.e., the repetition frequency of the femtosecond comb stabilized by an optical transition.[10] This optical frequency standard is based on an iodine-stabilized Nd:YAG laser at 1064 nm with an instability of $\sim 4 \times 10^{-14}$ at 1 s, and this optical frequency has been transferred from JILA to NIST by use of the second fiber. With independent femtosecond frequency combs operating in both laboratories, the absolute optical frequency can be measured simultaneously with reference to the common maser-based rf standard. A direct optical frequency comparison enabled by the fiber link has also been carried out, with results that are clearly superior to the rf-based measurements. We also include measurements of the degradation of the optical and rf standards that are due to the instability in the transmission channel. Active frequency-noise cancellation over the 6.9-km-long round-trip link has been developed, with optical frequency transfer instability between JILA and NIST through the BRAN fiber now reaching 3×10^{-15} at 1 s after noise cancellation. A unique aspect of the optical phase noise compensation reported in this study is that the transit time of the optical link is comparable with the coherence time of the laser, leading to interesting coherence effects. Entering into the details of this paper, we first give a brief introduction to the BRAN fiber, and we then discuss the work on transfer and measurement of rf standards in Section 2 and the optical standards in Section 3. Active fiber noise cancellation is discussed in Section 4.

The BRAN links the University of Colorado with some of Boulder's federal and other research laboratories and city offices through single-mode optical fiber. The 96-fiber bundle is installed in underground conduits and steam tunnels in an urban area and has an overall length of approximately 11 km. The BRAN fiber itself has a depressed cladding structure and is single mode at 1.3 μm, with the zero-dispersion wavelength near 1.3 μm and an attenuation coefficient at 1.3 μm of approximately -0.4 dB/km, according to the manufacturer. The network is divided into multiple sections that range from a few hundred meters to a few kilometers. Fibers in different sections of the network are connected with fiber-optic connectors at breakout panels located at various points of the network. When measured with an optical time-delay reflectometer, these interconnecting points reveal themselves by the sharp spikes in the reflection signal. Figure 1 shows such an optical time-delay reflectometer measurement on the two designated fibers that link JILA

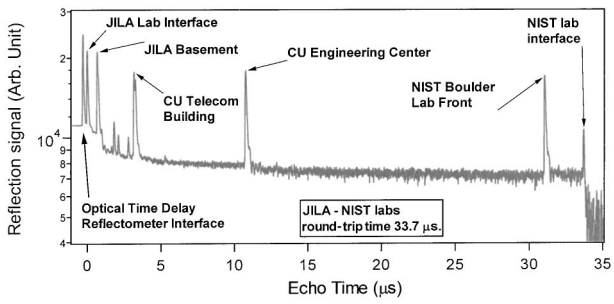

Fig. 1. Optical time-delay reflectometer measurement of the fiber link between JILA and NIST Boulder laboratories, showing the various interconnects along the link as exposed in the peaks of the reflected signal. The round-trip distance between the respective JILA and NIST laboratories is 6.89 km.

and NIST, displaying a number of round-trip times associated with the distances of the various interfaces from the JILA measurement origin. It is clear from the figure that the link between the JILA laboratory and the NIST laboratory is ~3.45 km long, and it includes four main junction boxes. The optical loss at 1.3 μm for the JILA–NIST–JILA round trip is −13 dB, most of which comes from the connections at these junction boxes.

2. TRANSMISSION OF RADIO FREQUENCY STANDARDS

The transmission of a hydrogen maser-based rf standard from NIST to JILA is accomplished by amplitude modulation of the light from a laser diode before it is launched into the BRAN fiber from a transmitter, as shown in Fig. 2. A high-power (30-mW) single-mode distributed-feedback laser, lasing at 1.3 μm, serves as the light source. The light is first coupled into an optical fiber and then into a high-speed, Mach–Zehnder modulator capable of intensity modulation of the light with a rf signal at frequencies up to 12 GHz. Part of the light that exits the modulator is split off by use of a coupler so that the dc intensity, and also the modulation signal being sent into the fiber, can be monitored. The bias on the modulator is set such that half of the dc optical power is transmitted. The bias point is stabilized to the half-power point by use of an active servo (see Fig. 2, inset). Under typical conditions, the dc optical power sent into the fiber is a few milliwatts, modulated from approximately 750 MHz to 1 GHz with a modulation index of approximately 10%. The rf signal is derived from a low phase-noise rf synthesizer that is referenced to the NIST ST-22 hydrogen maser. The value of the NIST synthesizer frequency can be set remotely from JILA by use of a web-based automation program.

To monitor the fiber-induced phase and frequency noise in the transmitted rf signal, we directly compare the original rf signal at NIST with the one that goes through the NIST–JILA–NIST round trip. The comparison is performed by use of two approaches: (1) by homodyne detection of the phase difference between the round-trip signal and the original source signal, and (2) by counting the frequency of a heterodyne beat between the round-trip signal and the original signal that has been frequency shifted by 10 kHz with a single-sideband-generation rf interferometer. Figure 3 presents a 16-h record of the output (left vertical axis) from a phase detector (a doubly balanced mixer). The slow time variation of the measured phase difference is much less than π and is consistent with the phase change expected from an ~0.25 °C variation of the fiber temperature over the same time window. For the 1-GHz modulation frequency used in this particular measurement, the long-term phase ramping would lead to a fractional frequency shift of $<2 \times 10^{-15}$. We also note that phase variations of smaller amplitudes but on much shorter time scales could lead to a larger fractional frequency offset during those particular measurement periods. Hence we have converted the phase variation record into the associated fractional frequency changes by differentiating the phase against time. The result is also presented in Fig. 3 by use of the right vertical axis. The fractional frequency changes are normally less than $\sim 4 \times 10^{-14}$.

Frequency-counting results are displayed in Fig. 4 in the form of the Allan deviation.[13] For this experiment, the original rf signal is split into two copies, one takes a round trip through the fiber media, while the other is sent into a single-sideband-generation rf interferometer to shift its frequency by 10 kHz. The heterodyne beat between the two signals produces a 10-kHz signal that is suitable for high-resolution frequency counting. Two sets of data are included under identical experimental conditions, except that in the first case, a 2-m-long fiber is used, whereas the BRAN fiber is used in the second case.

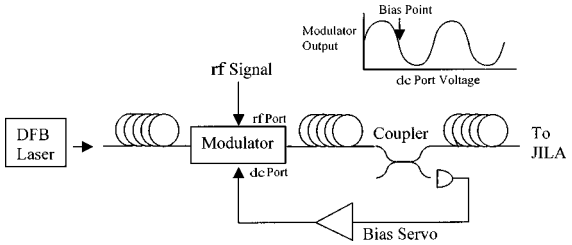

Fig. 2. Schematic of the rf transmission system from NIST to JILA. The inset shows the actively maintained dc bias point for the light power launched into the BRAN fiber.

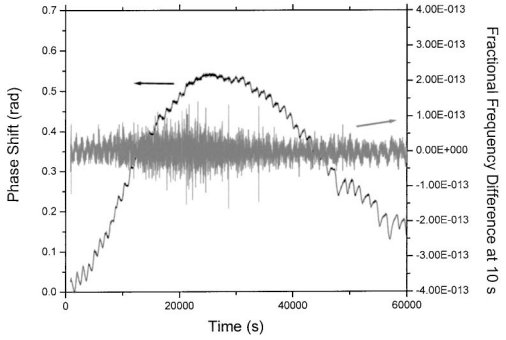

Fig. 3. Dark curve indicates the homodyne detection of phase fluctuations in the NIST–JILA–NIST fiber transmission channel taken over a 16-h period. The corresponding fractional frequency change of the 1-GHz rf signal is also shown with respect to the right vertical axis for an averaging time of 10 s.

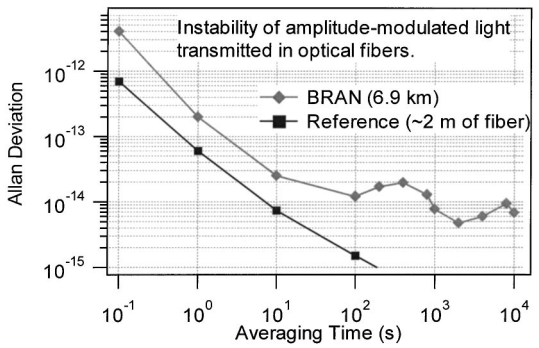

Fig. 4. Measured instability of amplitude-modulated light transmitted through a short (~2-m) fiber (squares) and through a round trip of the BRAN fiber (diamonds). The rf modulation signal carried by the fiber-transmitted light is heterodyne detected against the original signal source, which has been frequency shifted by 10 kHz by means of a single-sideband-generation rf interferometer.

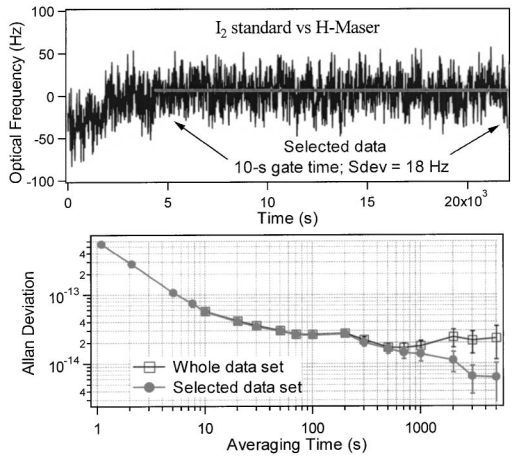

Fig. 5. Measured instability between the JILA iodine standard and the transmitted hydrogen maser-based signal from NIST by use of a femtosecond frequency comb. Top panel shows the measured optical frequency for a 10-s gate time and the bottom panel shows the associated Allan deviation.

The short fiber measurement allows one to evaluate the instability level of the rf modulation and detection system, shown as squares in Fig. 4. The added noise that is due to the BRAN fiber transfer can be clearly seen in Fig. 4, represented by the vertical offset between the diamonds and the squares. This fiber-induced additional fractional frequency noise is approximately 2×10^{-13} at 1-s averaging time and $1-2 \times 10^{-14}$ between 100 and 1000 s for a rf signal transfer by amplitude modulation of an optical carrier.

The transmitted maser-based rf signal is received at JILA by a fast Ge avalanche photodiode followed by appropriate signal conditioning. The resulting signal-to-noise ratio (SNR) of the rf signal is typically more than 70 dB in a 300-kHz bandwidth and is sufficiently high for the intended use as one of the main rf standards at JILA. This maser-based rf reference is more stable than most of the JILA rf standards, including a Rb atomic clock, a Cs atomic clock, and a stable low-phase-noise quartz oscillator. These rf signals have served as references for stabilization of the repetition frequency (f_{rep}) of the femtosecond laser comb used for absolute optical frequency measurements.[14–16] They have also been used for frequency comparisons against optically derived rf signals through the femtosecond comb.[10]

A diode-pumped all-solid-state Nd:YAG laser stabilized on an I_2 hyperfine transition at 532 nm has a demonstrated frequency instability of $\sim 4 \times 10^{-14}$ at 1 s. By referencing to the maser standard, the comb-based frequency measurement of this optical transition produces a significant improvement over the previous Cs-based work, although the maser's instability still limits the measurement precision at the short term.[12] Figure 5 displays a record (>6 h) of the optical frequency measurement with a (fiber-transferred) maser-referenced 750-MHz femtosecond optical comb. The initial drift seen in the data of the top panel was related to the changing residual amplitude modulation present in the (frequency-) modulation-transfer-based saturated absorption I_2 spectrometer. With the residual amplitude modulation stabilized, the frequency measurement result becomes rather stable, as indicated by the data after ~4000 s. Allan deviations (beyond 10-s averaging time) determined from the data in a juxtaposed manner are shown in the bottom panel, with the result represented by filled circles corresponding to the selected stable data and the open squares to the whole data set. Allan deviations for averaging times below 10 s are obtained from separate data runs where the measurement times correspond to the actual counter gate times. The measured instability at 1 s is 5.4×10^{-13}, slightly higher than the values shown in Figs. 4 and 6. However, a longer gate time quickly averages away the white phase noise presented in the beat, in a $1/\tau$ fashion, up to 10 s. We also note that the instability level at the averaging times of 100–1000 s is similar to that shown in Fig. 4, although in Fig. 5 only the one-way part of the fiber-induced phase noise plays a role in the measurement instability.

Instead of supplying a rf standard to stabilize the f_{rep} of the femtosecond comb, one can also use an optical frequency standard to stabilize f_{rep}, thus establishing an optically based atomic clock. We have indeed derived such a rf signal in f_{rep} from the I_2 optical standard. (For a detailed discussion of an I_2 optical clock, refer to Ref. 10). An ideal situation would be if the rf signal derived from the optical standard possessed the same level of stability as that of the optical standard itself. In other words, the transfer process from the optical to the rf domain should introduce only negligible noise. This situation can be probed by building two femtosecond comb systems that are referenced to the same high-quality optical frequency standard. Heterodyne beat in the optical domain and the rf domain would be expected to produce the same level of stability in an ideal situation. Tests along this line are ongoing at NIST.[17,18] On the other hand, a maser-based rf standard can already provide a useful check of the quality of an optical clock at the 10^{-13} and 10^{-14} levels. The

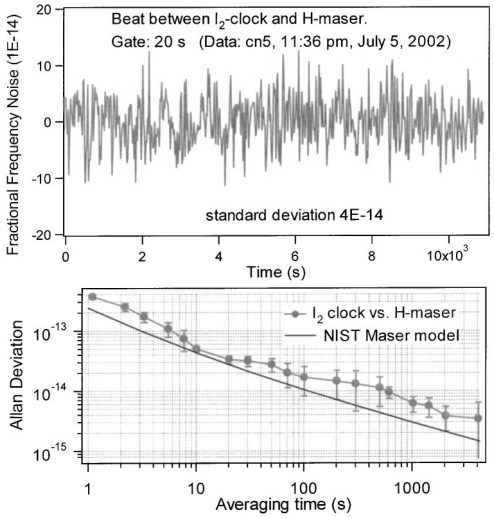

Fig. 6. Top panel, 3-h time record of the beat frequency between the BRAN-delivered maser-based signal and the f_{rep} of a femtosecond comb stabilized to an I_2-based optical frequency standard (I_2 optical clock). Bottom panel, corresponding Allan deviation determined from a few such beat records. (Data for the averaging times between 1 and 20 s were obtained from separate beat records with correspondingly varying gate times.) The NIST maser model is also shown.

top panel in Fig. 6 shows the recorded beat frequency between the BRAN-delivered maser signal and the JILA I_2 optical clock that runs continuously over several hours. We have accumulated a few such beat records, and the averaged Allan deviation is shown in the bottom panel of Fig. 6, starting from the 20-s averaging time in a juxtaposed manner. At shorter averaging times, below 20 s, we find it is important to use counter gate times that correspond to the actually quoted averaging times to avoid dead-time-related sampling noise. It is again noted that the Allan deviation between 100 and 1000 s is similar to those reported in Figs. 4 and 5.

3. TRANSMISSION OF OPTICAL FREQUENCY STANDARD

The BRAN fiber link also allows parallel transmission of the I_2-based optical frequency standard from JILA to NIST, along with the rf signal transfer. Of course, the wavelength of the Nd:YAG laser at 1.06 μm, which is below the cutoff wavelength for single-mode propagation in the fiber, is not ideal for the BRAN fiber transmission. Only approximately 5% of the launched optical power is delivered to NIST from JILA after additional losses at connectors and splices. However, the available power is enough for optical frequency measurements by use of a femtosecond comb system at NIST,[19] which can be carried out simultaneously with measurements at JILA. Although running at different repetition frequencies, both JILA and NIST femtosecond comb systems use maser-based signals for f_{rep} stabilization. Figure 7 presents simultaneous frequency measurement of the I_2 optical standard at both JILA and NIST. The JILA part of the data is the same as that shown in the beginning section of the top panel in Fig. 5. The agreement in frequency measurement over the entire measurement period between the two different comb systems linked by the BRAN fiber maser signal is ~2 Hz (a fraction of 7×10^{-15} of the measured optical frequency), with a statistical uncertainty of 28 Hz, in large part caused by the I_2 drift. However, if only the data measured simultaneously (within 10 s) are compared, the difference between the two comb results is 0.74 Hz, with a standard deviation of 9.1 Hz, limited basically by the averaging time. This result represents a significant improvement over our previous effort of coordinated JILA and NIST comb measurements by use of a GPS-corrected Cs clock for f_{rep} stabilization. In the earlier work the disagreement between the two comb measurements was at the level of a few tens of hertz, limited by the impractically long averaging times needed to reach the high precision level, starting from 5×10^{-12} at 1 s with the Cs standard.

Another informative experiment is to compare the short-term instability of the JILA I_2 optical standard with that of the local oscillator of the single mercury-ion-based optical standard at NIST. The basic setup for this test is shown in Fig. 8. A highly cavity-stabilized dye laser at 563 nm (532 THz) with a linewidth of less than 1 Hz (Ref. 5) serves as the optical reference for the frequency comb at NIST. The frequency-doubled output of this laser is used to probe the 6-Hz-wide optical transition of the trapped Hg^+. With the linear drift removed, the short-term (1–10-s) fractional frequency instability of this cavity-stabilized laser is $\leqslant 5 \times 10^{-16}$. Transmission of this stable light through a 180-m-long optical fiber to the femtosecond laser apparatus broadens its linewidth and increases its instability to the level of 4×10^{-15} for measurement times of 1–100 s, beyond which point the fiber-induced fluctuations begin to average down approximately as $1/\tau$.[9] A Doppler cancellation scheme similar to that employed on the much longer 3.45-km BRAN fiber link has been implemented (see Section 4) that effectively reduces the fiber-induced fluctuations to the level of $1 \times 10^{-17}/\tau$. However, for the measurements presented in this section, it was not necessary to employ the noise-cancellation servo for either fiber system.

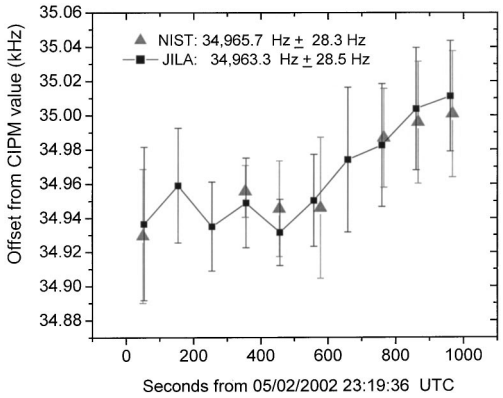

Fig. 7. Simultaneous femtosecond comb-based measurements of JILA's iodine standard versus the NIST maser reference. Measurements made at JILA and NIST both use 10-s gate time per sample, averaged over ten samples. Agreement between the two measurements is within 0.74 Hz, with a standard deviation of 9.1 Hz at 100-s averaging time. The most likely cause of instability between the two comb measurements is due to the noise introduced by the transmission of the maser reference frequency. (CIPM: International Committee for Weights and Measures.)

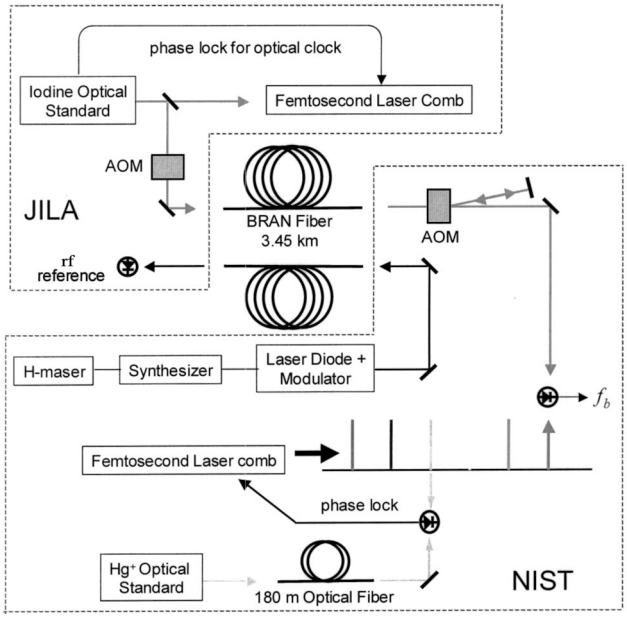

Fig. 8. Experimental setup for comparison of two remotely located optical frequency standards with the NIST femtosecond comb as the flywheel. The rf transmission channel is also shown.

The connection across the 250-THz frequency gap between the Hg^+ and the I_2 optical standards is provided by a broadband femtosecond-laser-based optical frequency comb. The frequency f_n of any tooth of this frequency comb can be expressed as $f_n = f_o + nf_{rep}$, where n is an integer, f_{rep} is the spacing of the comb elements, and f_o is an offset common to all elements. We used the self-referencing technique[20,21] to determine f_o, which is then phase locked to a stable rf signal synthesized from the hydrogen maser. With f_o fixed in this manner, we control the comb's other degree of freedom (f_{rep}) by measuring and phase locking the heterodyne beat between one element of the comb at 563 nm and the optical local oscillator for the Hg^+ standard.

Once the frequency comb is controlled by the Hg^+ local oscillator, an optical heterodyne beat between another element of the comb at 1064 nm and the I_2 standard is counted and recorded. During these measurements the cavity-stabilized optical local oscillator for Hg^+ was not locked to the ion transition itself. The drift associated with the local oscillator (that is due to the optical reference cavity) was calibrated by the maser and removed from the measurement. The SNR of the optical beat was observed to fluctuate between 10 and 30 dB (in 300-kHz bandwidth) as the birefringence of the BRAN fiber link drifted. We therefore used a voltage-controlled oscillator to track this beat to provide a constant amplitude signal for reliable counting. The resultant counting record of this optical heterodyne beat frequency is displayed as filled circles in the top panel in Fig. 9. A 10-kHz heterodyne beat between the stabilized f_{rep} at NIST and a stable rf signal synthesized from the hydrogen maser is also recorded with a frequency counter, with the result shown as open circles in the same top panel. The bottom panel shows the Allan deviation determined, respectively, from the two data sets, indicated by the same symbols as in the top panel. For comparison, we also included the Allan deviation (shown as open squares) determined from heterodyne beats between two similar I_2 standards at JILA. It is satisfactory to observe that the two optical diagnostics of the I_2 standard are in such close agreement. We can illustrate the stability advantage one gains in using optical standards by comparing the optical-based measurement to the microwave-based measurement. We also note that, although the BRAN fiber transmission involves no active noise cancellation for this particular experiment, the passive stability of the 3.45-km-long fiber is apparently just good enough to support the transmission of the I_2 optical standard.

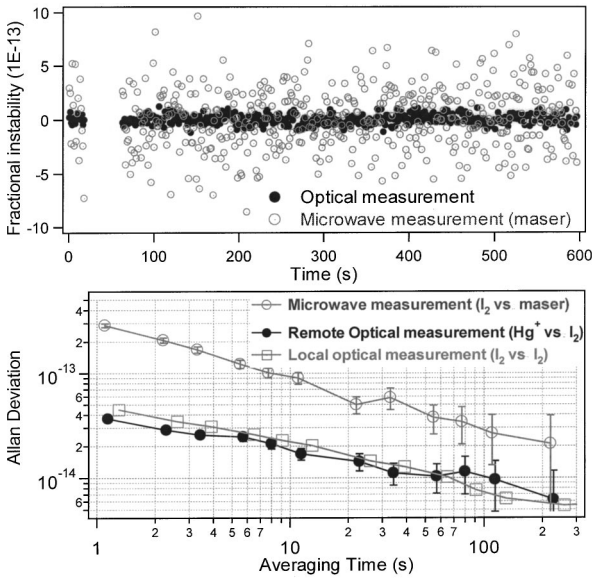

Fig. 9. Optical measurement between the I_2 and the Hg^+ standards is shown as filled circles and the maser-based rf measurement of the optical standard is shown as open circles. Top panel, time records of the beat frequency; bottom panel, the associated Allan deviations.

The additional instability associated with the fiber transmission of the optical carrier is not revealed in the above measurement. A direct heterodyne beat measurement between the outgoing and the returned optical signals finds a transmission (JILA–NIST–JILA) instability of $\sim 7.5 \times 10^{-15}$ for the optical carrier at 10-s averaging time (see Fig. 12 in Section 4). This transmission instability is approximately three times lower than that associated with the rf signal transfer, which is measured (at 10 s) to be $\sim 2.5 \times 10^{-14}$ for the round trip (Fig. 4). We suspect that the rf modulation technique could suffer from some excess noise associated with differential phase shifts between the optical carrier and its sidebands. We plan to carry out further measurements to confirm this hypothesis. Table 1 lists an instability budget for some of the elements in the system, all measured at 10-s averaging time.

4. ACTIVE CANCELLATION OF FIBER-INDUCED OPTICAL PHASE NOISE

Stability and accuracy of optical frequency standards are expected to advance to unprecedented levels in the near

Table 1. Instabilities of Various Elements in the Fiber-Transfer System, All Measured at 10-s Averaging Time

Elements	Instability
I_2 optical standard	2×10^{-14} (Fig. 9)
Hg^+ local oscillator	5×10^{-16} (independently verified)
Optical transfer (JILA–NIST–JILA)	7.5×10^{-15}; 1.3×10^{-15} (stabilized) (Fig. 12)
Synthesizer (tracking)	1.5×10^{-14} (independently verified)
NIST maser ST-22	4×10^{-14} (independently verified)
Maser transfer (NIST–JILA–NIST)	2.5×10^{-14} (Fig. 4)
Maser transfer (NIST–JILA)	2×10^{-14} (Fig. 6)

future.[22] To accommodate the need for effective distribution and comparison of these standards, active cancellation of fiber-induced phase noise should be explored to improve the transfer process. One avenue is to actively measure and cancel the noise on the rf signal that is used in the modulation process of an optical carrier. This is the approach adopted in the NASA work.[2] However, with the availability of the femtosecond comb system, it is now entirely practical and even advantageous to use an optical frequency itself as the carrier of the time and frequency information. One can employ the demonstrated high-accuracy comb systems at the two ends of the fiber to derive the rf signals, if necessary. Some intercomparisons can be performed entirely in the optical domain, such as the one described in Section 3. In this case it is the optical phase that needs to be stabilized. As pointed out in Section 1, such a Doppler cancellation scheme exists, with demonstrated performance in laboratory settings that shows the effective removal of optical phase-noise down to the measurement resolution. Work with BRAN fiber illustrates some of the possibilities and challenges one encounters in a longer fiber link that traverses a typical urban setting.

Figure 10 shows a simplified schematic of active fiber cancellation of optical phase noise induced by the BRAN fiber. The goal is to deliver the optical signal from JILA to NIST with stable and long-term phase coherence. Because of the low transmission efficiency of the fiber at 1.064 μm, we phase lock a second Nd:YAG laser to the one that is stabilized on the I_2 transition to provide a sufficient amount of power from the second laser for launch into the fiber. However, the input power to the fiber is typically set around 70 mW, limited by Brillouin backscattering, which has a threshold near 90 mW. The single-pass transmission efficiency for the launched power is approximately 5%.

For noise processes that are stationary relative to the light travel time, the fiber phase noise accumulated over one round trip is twice that for a one-way transit. We use this fact to detect and cancel the fiber phase noise. To isolate the signal returned from the remote end we encode it at the far end by shifting the optical carrier frequency by a known amount using an acousto-optic modulator (AOM 2). At the source end we then detect the heterodyne beat between the returned light and the outgoing laser beam into the fiber. Because BRAN is not a polarization-maintaining fiber, this beat signal shows a certain amount of fluctuation in amplitude. We therefore use a rf tracking filter, consisting of a voltage-controlled oscillator and a digital phase-locked loop, to regenerate a stable beat signal. If we feed this beat signal, which contains the round-trip phase noise, into the AOM in front of the fiber (AOM 1), with a negative sign, we cancel the round-trip phase noise and we can recover a clean optical signal back at JILA after the JILA–NIST–JILA round trip. If we instead feed only half of the phase information contained in the beat signal (this can be accomplished by a digital frequency divider), again with a negative sign, into AOM 1, then at the remote end at NIST we will be able to recover a clean optical signal, ideally an exact copy of what is sent into the fiber at JILA.

To verify that this fiber cancellation scheme indeed accomplishes the desired goal, we first test the effect of cancellation of the round-trip phase noise. This task is more straightforward to carry out, as all tests can be done at the fiber input end. We start by analyzing the linewidth of a heterodyne beat signal between the original laser beam (before AOM 1) and the returned light. Of course the delayed self-heterodyne technique is an established method for laser linewidth measurement when the delay time far exceeds the laser field coherence time. At the other extreme, when the delay time is much shorter than the laser coherence time, then the beat linewidth is basically represented by a spectral delta function, modulated by delay time fluctuations in the fiber loop. When the delay time and the laser coherence time are comparable, the beat line shape takes the form of a spectral delta function sitting on top of a modified Lorentzian pedestal. This last situation corresponds to our experimental condition for which both the fiber round-trip delay and the laser coherence time are ~33 μs. However, because of the phase noise accumulated during the 6.9-km round trip through the BRAN fiber, the central delta function component is broadened to approximately 2 kHz. This effect is shown as the dotted curve in Fig. 11, where a fast Fourier transform signal analyzer has been employed to reveal the linewidth of the heterodyne beat signal. We obtained the 50-kHz line-center frequency of the signal by mixing the optical heterodyne beat with an appropriately tuned auxiliary rf signal. This step of signal processing is necessary for enhanced resolution in the spectral analysis. When the fiber noise-cancellation system is activated, we recover a narrow spectral peak on top of the pedestal, as shown in Fig. 11. Within the cancellation servo bandwidth of ~3 kHz, the laser field is mainly coherent on the time scale of the fiber delay, and so the noise cancellation acts primarily on the fiber-induced noise. However, for noise processes that have faster Fourier frequencies, the cancellation servo loop can actually mistakenly interpret the laser noise as if it were the fiber noise. The result is the increased noise level at these higher Fourier frequencies, leading to the formation of a pedestal. One can appreciate the effect of fiber noise cancellation if we take a high-resolution scan of the beat spectrum. As the inset in Fig. 11 indicates, when we zoom in around the beat signal with a full span of only 1 kHz and a resolution bandwidth of 0.048 Hz, we observe only a white-noise floor when the round-trip fiber noise is not cancelled. If we turn on the active noise cancellation, we recover a sharp coherent linewidth of 0.05 Hz, essentially limited by the

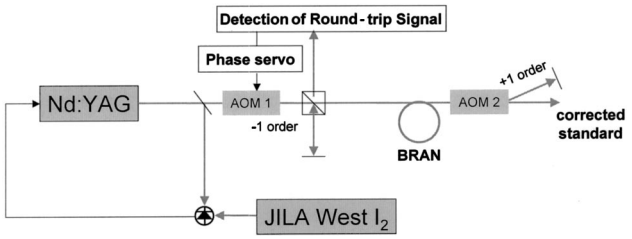

Fig. 10. Active cancellation of the optical phase noise induced by the BRAN fiber. The first-order diffracted beam is used after each AOM. The phase servo electronics can provide accurate cancellation of the single-pass fiber phase noise, based on the measured round-trip deviations.

analyzer resolution bandwidth. It is satisfying to see the good SNR of the beat even though one would expect that the close-in noise near the carrier would be exposed by such a small resolution bandwidth. We also deliberately put noise on the original laser to further decrease its coherence time. This leads to further broadening of the pedestal without any effect on the coherent peak in the middle. The peak height can be reduced, of course, because of the spread of the central carrier power to the noise sidebands in the pedestal.

Frequency counting of the heterodyne beat signal is also recorded, with the results shown in Fig. 12. The top panel at left shows a counting standard deviation of 5.4 Hz at a 1-s counter gate time, when the fiber noise is uncompensated. The bottom panel shows the counting record when the fiber noise is canceled, now with a standard deviation of 0.9 Hz. Allan deviations determined from these two time records are shown at right in Fig. 12. After phase compensation, the round-trip transfer process exhibits an instability of 3×10^{-15} at 1-s integration time and averages down $\sim\tau^{-1/2}$. We emphasize that such

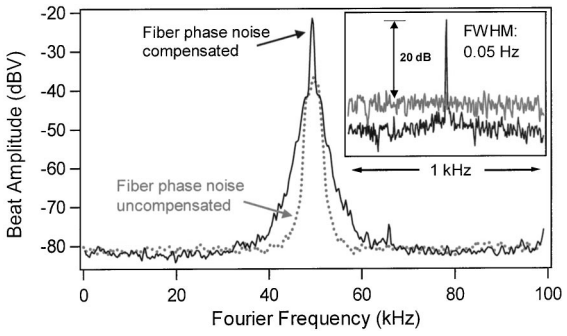

Fig. 11. Fourier spectral analysis of the heterodyne beat linewidth between the original laser beam (before AOM 1) and the returned light. Without phase compensation, the beat linewidth is broadened by the fiber to ~2 kHz. The inset shows the display of a beat signal at a 1-kHz span and a 0.048-Hz resolution bandwidth when the fiber noise cancellation is activated. This is in contrast with the white-noise floor that shows in the same spectral window when phase noise is not canceled. Note the lowered noise level that is due to the emergence of the recovered carrier signal when cancellation is activated.

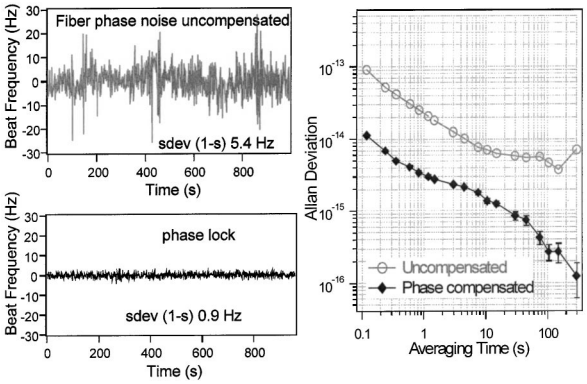

Fig. 12. Counted heterodyne beat signal between the original laser and the returned light after a round trip. The top left panel corresponds to the case when the fiber noise is uncompensated, and the bottom left panel shows the compensated case, both with a 1-s counter gate time. Allan deviations determined from the time records are shown at right.

performance is limited by the actual SNR available in the heterodyne beat, which is less than ideal in the present situation because of the mismatch between the fiber and the propagation wavelength.

We have also stabilized the one-way fiber transmission phase between JILA and NIST. However, our current experimental condition is not yet ready to reveal the benefit of such a system. As indicated by the Allan deviation of the uncompensated case in Fig. 12, the passive fiber transmission would support a stability measurement of $2-3 \times 10^{-14}$ at 1 s, which is actually slightly better than the stability of the present I_2 standard at JILA. With an improved I_2 system[23] and other highly stable optical standards such as Ca or Hg^+ at NIST, such a stable optical link between JILA and NIST will be indispensable.

5. CONCLUSIONS

Fiber-based communication networks will play an increasingly important role in dissemination of future time and frequency standards, in particular for the emerging optically based frequency standards and clocks. Our purpose in this paper was to document the coordinated efforts of JILA, NIST, and BIPM in transferring highly stable rf and optical frequency standards over an installed optical dark fiber link. To the best of our knowledge the work reported represents the first phase coherent transfer of an optical frequency standard over a commercial fiber link of kilometer-scale length. Active phase compensation is implemented to eliminate fiber-induced propagation noise and the resultant instability of the transfer process is limited to $\leqslant 3 \times 10^{-15}$ at 1-s averaging time. It is clear that, with the help of femtosecond comb systems, the direct use of an optical carrier for time and frequency distributions can be significantly more advantageous than the traditional modulation approaches in the rf domain. The transferred optical frequency signal can be measured directly and simultaneously at both the sending and receiving ends, representing a new class of coherent optical communication. Simultaneous use of the optical phase and rf modulation could also prove to be fruitful with new tools in mode-locked fiber lasers and diode lasers that operate within the telecommunication wavelength range.[24,25] In principle, a fiber-based active noise-cancellation system such as the one reported in this paper does not necessarily have to be restricted to a local area network. For example, if the active noise-cancellation bandwidth one employs is less than 100 Hz, which might be sufficient for fiber bundles buried in environmentally stable underground conduits, then 20 or so fiber noise-cancellation stations (let us call them coherence restoration repeaters) should be able to relay stable optical standards from Boulder, Colorado, to Washington D.C.

ACKNOWLEDGMENTS

We are grateful to J. Levine for many useful discussions and critical comments. We also acknowledge technical help from M. Notcutt, A. Marian, L. Chen, S. Foreman, S. T. Cundiff, C. Ishibashi, and T. Parker. This work is supported chiefly by the Multidisciplinary Research Program

of the University Research Initiative (MURI) for the development of optical atomic clocks, administered by the U.S. Office of Naval Research. Partial funding support comes also from NASA, the NIST, and the National Science Foundation. R. J. Jones is a National Research Council postdoctoral fellow. K. W. Holman is a John and Fannie Hertz Foundation graduate fellow. J. Ye and J. L. Hall are also staff members of the Quantum Physics Division of NIST Boulder.

*The corresponding authors, Jun Ye, can be reached by e-mail at Ye@jila.colorado.edu; or by telephone at 303-735-3171.

¶Present address: Center for Measurement Standards, 321 Kuang Fu Road, Hsinchu, Taiwan.

REFERENCES AND NOTE

1. J. Levine, "Introduction to time and frequency metrology," Rev. Sci. Instrum. **70**, 2567–2596 (1999).
2. M. Calhoun, R. Sydnor, and W. Diener, "A stabilized 100-megahertz and 1-gigahertz reference frequency distribution for Cassini Radio Science," in Interplanetary Network Progress Rep. 42-148, Oct.–Dec. 2001 (Jet Propulsion Laboratory, Pasadena, Calif., (15 February 2002), pp. 1–11.
3. T. P. Celano, S. R. Stein, G. A. Gifford, B. A. Mesander, and B. J. Ramsey, "Subpicosecond active timing control over fiber optic cable," *Proceedings of the 2002 IEEE International Frequency Control Symposium* (IEEE, New York, 2002), pp. 510–516.
4. L. S. Ma, P. A. Jungner, J. Ye, and J. L. Hall, "Delivering the same optical frequency at two places: accurate cancellation of phase noise introduced by an optical fiber or other time-varying path," Opt. Lett. **19**, 1777–1779 (1994).
5. B. C. Young, F. C. Cruz, W. M. Itano, and J. C. Bergquist, "Visible lasers with subhertz linewidths," Phys. Rev. Lett. **82**, 3799–3802 (1999).
6. R. J. Rafac, B. C. Young, J. A. Beall, W. M. Itano, D. J. Wineland, and J. C. Bergquist, "Sub-dekahertz ultraviolet spectroscopy of $^{199}Hg^{+}$," Phys. Rev. Lett. **85**, 2462–2465 (2000).
7. T. Udem, S. A. Diddams, K. R. Vogel, C. W. Oates, E. A. Curtis, W. D. Lee, W. M. Itano, R. E. Drullinger, J. C. Bergquist, and L. Hollberg, "Absolute frequency measurements of the Hg^{+} and Ca optical clock transitions with a femtosecond laser," Phys. Rev. Lett. **86**, 4996–4999 (2001).
8. B. deBeauvoir, F. Nez, L. Julien, B. Cagnac, F. Biraben, D. Touahri, L. Hilico, O. Acef, A. Clairon, and J. J. Zondy, "Absolute frequency measurement of the 2S-8S/D transitions in hydrogen and deuterium: new determination of the Rydberg constant," Phys. Rev. Lett. **78**, 440–443 (1997).
9. S. A. Diddams, T. Udem, J. C. Bergquist, E. A. Curtis, R. E. Drullinger, L. Hollberg, W. M. Itano, W. D. Lee, C. W. Oates, K. R. Vogel, and D. J. Wineland, "An optical clock based on a single trapped Hg-199(+) ion," Science **293**, 825–828 (2001).
10. J. Ye, L. S. Ma, and J. L. Hall, "Molecular iodine clock," Phys. Rev. Lett. **87**, 270801/1–4 (2001).
11. BRAN network, see http://www.branfiber.net/drawings/Bran6.gif.
12. R. J. Jones, W. Y. Cheng, K. W. Holman, L.-S. Chen, J. L. Hall, and J. Ye, "Absolute frequency measurement of the length standard at 514 nm," Appl. Phys. B **74**, 597–601 (2002).
13. D. W. Allan, "Statistics of atomic frequency standards," Proc. IEEE **54**, 221–231 (1966).
14. S. A. Diddams, D. J. Jones, J. Ye, T. Cundiff, J. L. Hall, J. K. Ranka, R. S. Windeler, R. Holzwarth, T. Udem, and T. W. Hänsch, "Direct link between microwave and optical frequencies with a 300 THz femtosecond laser comb," Phys. Rev. Lett. **84**, 5102–5105 (2000).
15. J. Ye, T. H. Yoon, J. L. Hall, A. A. Madej, J. E. Bernard, K. J. Siemsen, L. Marmet, J.-M. Chartier, and A. Chariter, "Accuracy comparison of absolute optical frequency measurement between harmonic-generation synthesis and a frequency-division femtosecond comb," Phys. Rev. Lett. **85**, 3797–3800 (2000).
16. J. Ye, J. L. Hall, and S. A. Diddams, "Precision phase control of ultrawide bandwidth fs laser-A network of ultrastable frequency marks across the visible spectrum," Opt. Lett. **25**, 1675–1677 (2000).
17. E. N. Ivanov, L. Hollberg, and S. A. Diddams, "Analysis of noise mechanisms limiting frequency stability of microwave signals generated with a femtosecond laser," in *Proceedings of the 2001 IEEE International Frequency Control Symposium* (Institute of Electrical and Electronics Engineers, Piscataway, N. J., 2001).
18. S. A. Diddams, L. Hollberg, L. S. Ma, and L. Robertsson, "Femtosecond-laser-based optical clockwork with instability $\leq 6.3 \times 10^{-16}$ in 1 s," Opt. Lett. **27**, 58–60 (2002).
19. S. A. Diddams, Th. Udem, K. R. Vogel, C. W. Oates, E. A. Curtis, R. S. Windeler, A. Bartels, J. C. Bergquist, and L. Hollberg, "A compact femtosecond-laser-based optical clockwork," in *Laser Frequency Stabilization, Standards, Measurement, and Applications*, J. L. Hall and J. Ye, eds., Proc. SPIE **4269**, 77–83 (2001).
20. D. J. Jones, S. A. Diddams, J. K. Ranka, A. Stentz, R. S. Windeler, J. L. Hall, and S. T. Cundiff, "Carrier-envelope phase control of femtosecond mode-locked lasers and direct optical frequency synthesis," Science **288**, 635–639 (2000).
21. R. Holzwarth, T. Udem, T. W. Hänsch, J. C. Knight, W. J. Wadsworth, and P. S. J. Russell, "Optical frequency synthesizer for precision spectroscopy," Phys. Rev. Lett. **85**, 2264–2267 (2000).
22. L. Hollberg, C. W. Oates, E. A. Curtis, E. N. Ivanov, S. A. Diddams, T. Udem, H. G. Robinson, J. C. Bergquist, R. J. Rafac, W. M. Itano, R. E. Drullinger, and D. J. Wineland, "Optical frequency standards and measurements," IEEE J. Quantum Electron. **37**, 1502–1513 (2001).
23. W.-Y. Cheng, L. S. Chen, T. H. Yoon, J. L. Hall, and J. Ye, "Sub-Doppler molecular-iodine transitions near the dissociation limit (523–498 nm)," Opt. Lett. **27**, 571–573 (2002).
24. J. Rauschenberger, T. M. Fortier, D. J. Jones, J. Ye, and S. T. Cundiff, "Control of the comb from a modelocked Erbium doped fiber laser," Opt. Express **10**, 1404–1409 (2002), http://www.opticsexpress.org.
25. D. J. Jones, K. W. Holman, M. Notcutt, J. Ye, J. Chandalia, L. Jiang, E. Ippen, and H. Yokoyama, "Ultra-low jitter, 1550-nm mode-locked semiconductor laser synchronized to a visible optical frequency standard," Opt. Lett. **28**, 813–815 (2003).